A large magmatic sill complex beneath the Toba caldera

K. Jaxybulatov *et al.*

Science **346**, 617 (2014);
DOI: 10.1126/science.1258582

Science (print ISSN 0036-8075; online ISSN 1095-9203) is published weekly, except the last week in December, by the American Association for the Advancement of Science, 1200 New York Avenue NW, Washington, DC 20005.

Recherche Scientifique and Commissariat a l'Energie Atomique, the French-American Cultural Exchange, the Italian Istituto Nazionale di Fisica Nucleare, the National Research Foundation of Korea, and the UK's Science and Technology Facilities Council. Jefferson Science Associates operates the Thomas Jefferson National Accelerator Facility for the DOE, Office of Science, Office of Nuclear Physics under contract DE-AC05-06OR23177. The raw data from this experiment are archived in Jefferson Lab's mass storage silo.

SUPPLEMENTARY MATERIALS

www.sciencemag.org/content/346/6209/614/suppl/DC1
Materials and Methods
Figs. S1 to S30
Tables S1 to S8
References (*40*–*51*)

2 June 2014; accepted 2 October 2014
Published online 16 October 2014;
10.1126/science.1256785

VOLCANOLOGY

A large magmatic sill complex beneath the Toba caldera

K. Jaxybulatov,[1,2,3] N. M. Shapiro,[3]* I. Koulakov,[1,2] A. Mordret,[3] M. Landès,[3] C. Sens-Schönfelder[4]

An understanding of the formation of large magmatic reservoirs is a key issue for the evaluation of possible strong volcanic eruptions in the future. We estimated the size and level of maturity of one of the largest volcanic reservoirs, based on radial seismic anisotropy. We used ambient-noise seismic tomography below the Toba caldera (in northern Sumatra) to observe the anisotropy that we interpret as the expression of a fine-scale layering caused by the presence of many partially molten sills in the crust below 7 kilometers. This result demonstrates that the magmatic reservoirs of present (non-eroded) supervolcanoes can be formed as large sill complexes and supports the concept of the long-term incremental evolution of magma bodies that lead to the largest volcanic eruptions.

The size and type of a volcanic eruption depend on the processes that occur in the magmatic reservoirs in Earth's crust. In particular, the largest eruptions require the building of extended pools of viscous gas-rich magma within the crust (*1*–*3*). In the present study, we investigated the magmatic system that produced one of the strongest eruptions in the Quaternary: the Toba event that occurred 74,000 years ago in northern Sumatra, Indonesia (Fig. 1), and emitted at least 2800 cubic kilometers of volcanic material (*4*). This catastrophe is believed to have affected the global climate and to have had a strong impact on the biosphere (*4*, *5*). The event was preceded during the previous 2 million years by at least four other eruptions in nearby locations that had volcano explosivity indices above 7 (*4*). The generation of this exceptional sequence of eruptions could be possible with the existence of a very large magma reservoir in the crust that formed over a long period of time (>1 million years) (*6*). Considering the relatively short period of time that has passed since the main Toba event, the structures that were responsible for the formation and functioning of this reservoir are expected to be well preserved in the Sumatra crust to date. Combined with previous geophysical investigations, the new data presented here provide us with information about the structure of the Toba volcano-magmatic complex and help us to better understand the internal structure and ascent mechanism of large magma volumes through the crust before their super-eruptions.

Geological observations of eroded and exposed past volcanoes and geodynamic models indicate that volcano-magmatic reservoirs evolve over long periods of time and grow in small increments, with the formation of dykes or sills (*2*, *3*, *7*–*9*). However, the exact mechanisms involved in the ascent and emplacement of the magma in the crust beneath active volcanoes are not yet completely understood, mainly because of the lack of detailed information about the structures of volcano-magmatic complexes below volcanoes in their most productive phase. Large-scale images of zones affected by melts can be obtained with magneto-telluric methods (*10*) and with seismic tomography (*11*). Some signatures of large crustal intrusions can also be detected by receiver functions (*12*). However, the individual dykes or sills within magmatic complexes that have metric or decametric thicknesses (*7*) cannot be deduced from geophysical imaging alone, and as layered intrusions, their interpretation requires additional geological information (*13*).

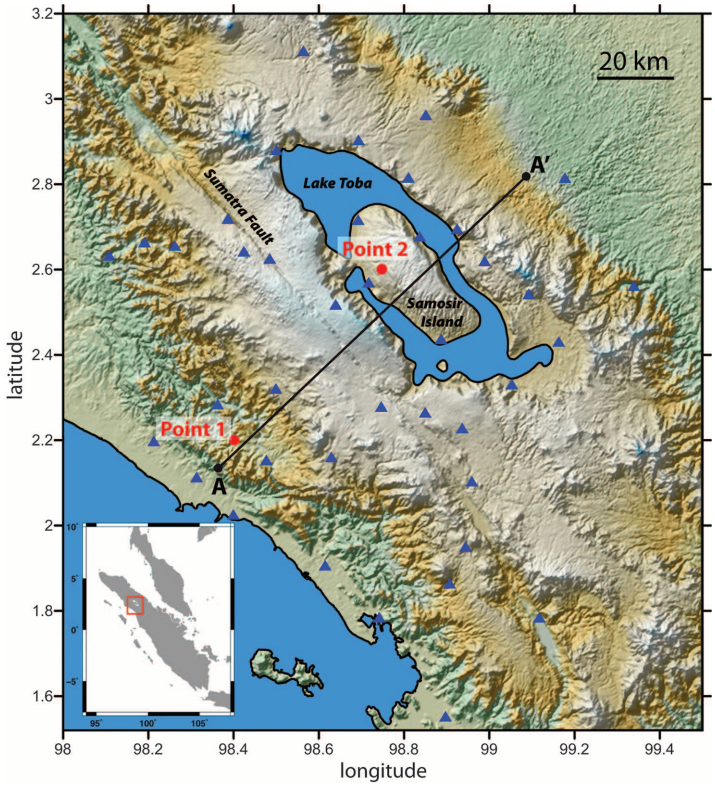

Fig. 1. Topographic map of the Lake Toba region. Blue triangles, locations of the seismic stations; black line, profile for cross sections shown in Fig. 3; red circles, locations where 1D inversion is illustrated in figs. S6 and S8. (Inset) Location of the Lake Toba region within northern Sumatra.

[1]Trofimuk Institute of Petroleum Geology and Geophysics, Siberian Branch of Russian Academy of Sciences, Prospekt Koptyuga, 3, Novosibirsk 630090, Russia. [2]Novosibirsk State University, 2, Pirogova Street, Novosibirsk 630090, Russia. [3]Institut de Physique du Globe de Paris, Sorbonne Paris Cité, CNRS (UMR 7154), 1 rue Jussieu, 75238 Paris, Cedex 5, France. [4]GFZ German Research Centre for Geosciences, Telegrafenberg 14473 Potsdam, Germany.
*Corresponding author. E-mail: nshapiro@ipgp.fr

Fine-scale layering in dyke or sill complexes affects the macromechanical properties of the crustal material, which results in anisotropy that can be measured with seismic waves. For example, the faster velocities of vertically propagating *P* waves below the Merapi volcano (Java, Indonesia) (*14*) were attributed to the presence of dykes with dominantly vertical orientations. Alternatively, the horizontal layering that is typical for sill complexes would result in so-called radial anisotropy (vertical transversely isotropic media with a vertical slow axis of symmetry) (*15*). This type of anisotropy is well known in the upper mantle, where it is mainly associated with mineralogical preferential orientation caused by the strain in response to large-scale mantle flow (*16*). Similar processes are believed to produce the radial anisotropy that has been observed recently within the crust in tectonically active regions (*17*, *18*). Transverse isotropy is also well known in sedimentary rock (*19*).

One of the methods used to estimate radial anisotropy is the measurement and simultaneous inversion of dispersion curves of Rayleigh and Love surface waves (*16*). Inferring information about crustal structure generally requires dispersion measurements at periods <20 s, which are now possible with methods based on the correlation of ambient seismic noise (*20*). We have applied noise-based surface-wave seismic tomography to study the structure of the middle and upper crust below the Toba caldera and its surrounding areas (*21*). Recent seismological studies (*22*–*25*) have indicated the presence of low–seismic-velocity anomalies beneath the Toba caldera that might be associated with sediments filling the caldera at its shallowest levels and with magma or partly molten portions in the deeper crust and mantle. However, because of poor vertical resolution, these seismic images have not provided indications to date about how these magma bodies might have been emplaced within the crust.

We processed continuous records from 40 seismic stations that were installed around Lake Toba (*25*) between May and October 2008 (Fig. 1) to compute the cross-correlations of ambient seismic noise (fig. S1). The resulting waveforms were used to measure group velocities of fundamental-mode Rayleigh and Love waves (*26*) at periods between 3 and 19 s. We then regionalized these measurements to obtain two-dimensional (2D) maps (Fig. 2) of the distribution of group velocities (*27*). A 3D model of the distribution of the shear speeds within the crust (Fig. 3) was constructed via inverting regionalized dispersion curves with a neighborhood algorithm (*21*, *28*).

For Rayleigh waves (Fig. 2, A and B, and fig. S9) at all periods, the group velocity distributions show the prominent low-velocity anomaly beneath Samosir Island, which is located in the central part of the Toba caldera. These images are similar to those previously obtained with the same data set but slightly different data processing and inversion (*25*), and they are consistent with the body wave tomography (*24*). For Love waves, the strong low-velocity anomaly is also observed for short periods that correspond to shallower depths (Fig. 2C), although its amplitude strongly decreases at long periods that are affected by deeper structures (Fig. 2D). To explain this difference between Rayleigh and Love waves, there is the need to introduce radial anisotropy (transverse isotropy with a vertical symmetry axis) with a horizontally polarized shear wave speed (V_{SH}) that is greater than the vertically polarized shear wave speed (V_{SV}). This anisotropy is required at depths >7 km (figs S6 to S8) below the Toba caldera, whereas outside this region, the data can be explained through an isotropic middle crust.

The radial anisotropy within the middle crust below the Toba caldera (fig. S9) can be explained by a large layered intrusion complex that is dominated by horizontally oriented sills (Fig. 3D). We have estimated the possible macromechanical properties of such media via the modeling of seismic velocities in random layered structures (*15*, *21*). We compared the modeling results with the average shear wave speeds V_{SV} and V_{SH} observed below the Toba caldera at depths between 7 and 20 km (~3.0 and ~3.35 km/s, respectively). We also used the regional tomographic model (*24*) that is based on records from earthquakes that were mainly located below the Toba caldera (i.e., on the nearly vertical rays) to deduce the average speed of the vertically propagating *P* waves (V_{PV}), which was approximately 5.3 km/s. After testing numerous random structures whose properties were based on the known seismic speeds of plutonic rock (*29*, *30*) and on typical thicknesses of sills (*7*), we found that the observed strong radial anisotropy and low V_{SV} can be explained by the presence of molten fractions in some sills (table S1), which is in agreement with geodynamic models (*2*).

Fast magma displacements and strong explosions during super-eruptions might destroy the dominant horizontal stratification in the uppermost crust. Based on our tomography images, we hypothesize that the observed nearly isotropic low-velocity anomaly above 7 km in depth beneath the caldera (Fig. 3D, red area above dotted line) represents the medium that was affected by the most recent Toba eruption, 74,000 years ago.

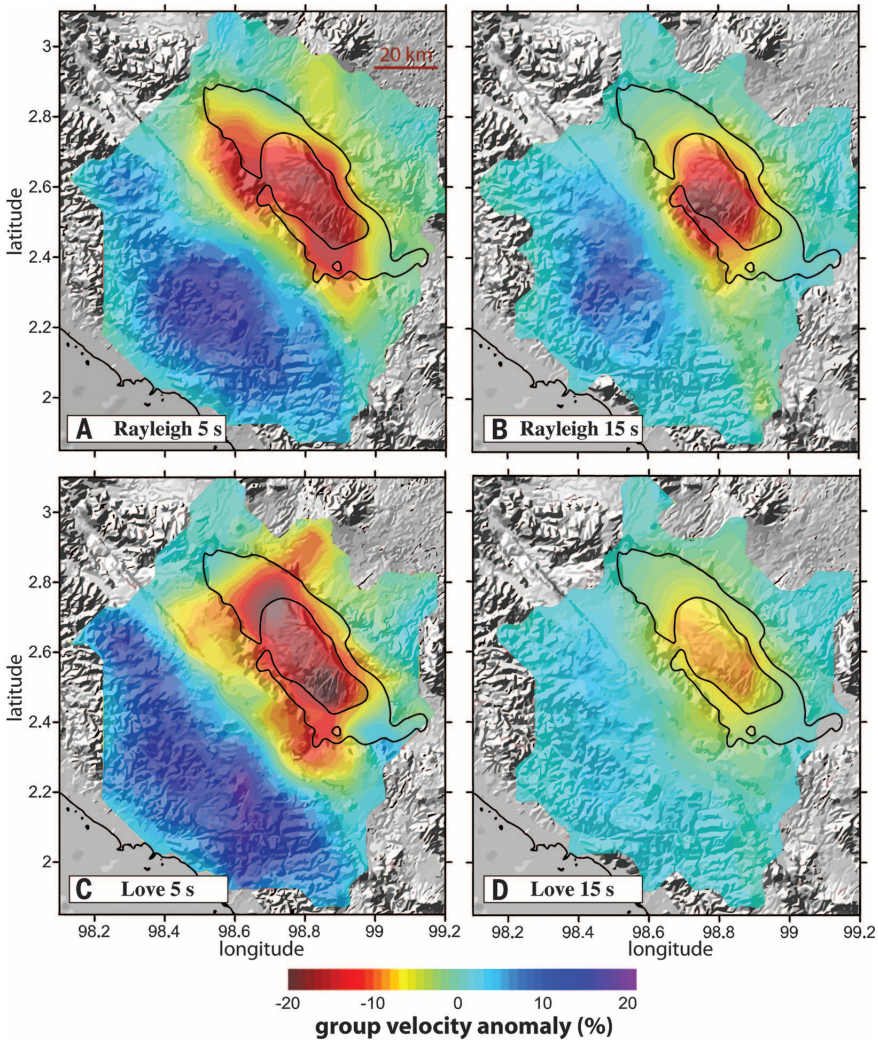

Fig. 2. Group velocity maps of the Rayleigh and Love waves derived from the ambient noise tomography. Colors plotted on top of the shaded relief show group velocity anomalies relative to average values at every period. (**A** and **B**) show Rayleigh wave maps, and (**C** and **D**) show Love wave maps.

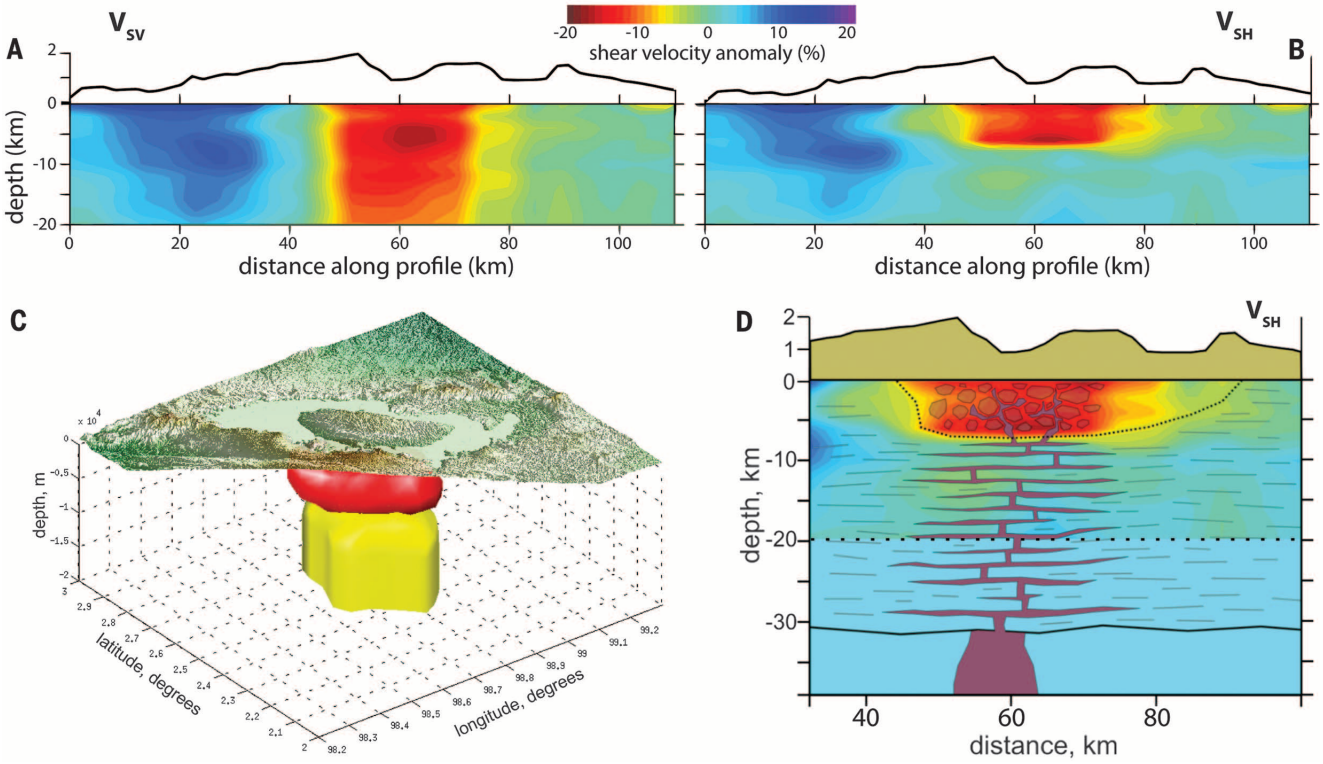

Fig. 3. 3D shear velocity model below the Toba caldera and its interpretation. (**A**) Distribution of V_{SV} in vertical cross section along profile A-A' of Fig. 1. The topography is vertically exaggerated. (**B**) Similar to (A), but for V_{SH}. (**C**) 3D iso-surface representation of the tomographic model. Red surface, low (<–10%) Voigt average speed anomaly; yellow surface, region with strong (>10%) radial anisotropy [$\xi = 2 \times 100\% \times (V_{SH} - V_{SV})/(V_{SH} + V_{SV})$]. Vertically exaggerated topography is shown on the top. (**D**) Schematic interpretation of the velocity structure for the Toba caldera complex superimposed on the distribution of the V_{SH} (shown above 20 km in depth). The anisotropy below 7 km in depth appears to be due to a layered magmatic intrusion dominated by horizontally oriented sills. Dotted line, the low-velocity area below the caldera that might have been affected by the super-eruption 74,000 years ago and where the horizontal stratification would not be preserved.

Below 7 km in depth, the strong horizontal anisotropy corresponds to the preserved sill complex in the middle crust.

The evidence obtained for significant crustal anisotropy, together with the information derived on Toba from other geophysical studies, provides the key to an understanding of the magma intrusion mechanisms that are related to large caldera-forming eruptions. These large-scale volcanic events, such as that of Toba 74,000 years ago, should be preceded by a massive ascent of a large volume of magma. A plausible scenario is that this magma was accumulated incrementally over long periods of time and mainly in the form of successive sill-type intrusions, as suggested by geodynamic models (*2*, *3*, *7*, *8*, *31*). This resulted in the formation of a large layered intrusion complex in the crust. The preferential horizontal orientation of the layers within this sill complex containing a significant amount of melt leads to the observed radial anisotropy. We argue, therefore, that observations of such anisotropy can be used to image and to characterize parts of the crust where the partially molten magma is accumulated before future eruptions.

REFERENCES AND NOTES

1. O. Bachmann, G. Bergantz, *Elements* **4**, 17–21 (2008).
2. C. Annen, J.-D. Blundy, R. S. J. Sparks, *J. Petrol.* **47**, 505–539 (2006).
3. C. Annen, *Earth Planet. Sci. Lett.* **284**, 409–416 (2009).
4. C. A. Chesner, *Quat. Int.* **258**, 5–18 (2012).
5. F. J. Gathorne-Hardy, W. E. H. Harcourt-Smith, *J. Hum. Evol.* **45**, 227–230 (2003).
6. J. E. Gardner, P. W. Layer, M. J. Rutherford, *Geology* **30**, 347–350 (2002).
7. C. Michaut, C. Jaupart, *Tectonophysics* **500**, 34–49 (2011).
8. A. Gudmundsson, *Tectonophysics* **500**, 50–64 (2011).
9. B. Taisne, C. Jaupart, *J. Geophys. Res.* **114**, B09203 (2009).
10. G. J. Hill *et al.*, *Nat. Geosci.* **2**, 785–789 (2009).
11. J. M. Lees, *J. Volcanol. Geotherm. Res.* **167**, 37–56 (2007).
12. X. Peng, E. D. Humphreys, *J. Geophys. Res.* **103**, 7171–7186 (1998).
13. J. W. Shervais, S. K. Vetter, B. B. Hanan, *Geology* **34**, 365–368 (2006).
14. I. Koulakov, A. Jakovlev, B. G. Luehr, *Geochem. Geophys. Geosyst.* **10**, Q02011 (2009).
15. G. W. Postma, *Geophysics* **20**, 780–806 (1955).
16. G. Ekström, A. M. Dziewonski, *Nature* **394**, 168–172 (1998).
17. N. M. Shapiro, M. H. Ritzwoller, P. Molnar, V. Levin, *Science* **305**, 233–236 (2004).
18. M. P. Moschetti, M. H. Ritzwoller, F. Lin, Y. Yang, *Nature* **464**, 885–889 (2010).
19. Z. Wang, *Geophysics* **67**, 1423–1440 (2002).
20. N. M. Shapiro, M. Campillo, L. Stehly, M. H. Ritzwoller, *Science* **307**, 1615–1618 (2005).
21. Information on materials and methods is available on *Science* Online.
22. R. Masturyono *et al.*, *Geochem. Geophys. Geosyst.* **2**, 1014 (2001).
23. K. Sakaguchi, H. Gilbert, G. Zandt, *Geophys. Res. Lett.* **33**, L20305 (2006).
24. I. Koulakov, T. Yudistira, B. G. Luehr, P. Wandono, *Geophys. J. Int.* **177**, 1121–1139 (2009).
25. J. Stankiewicz, T. Ryberg, C. Haberland, D. Fauzi, D. Natawidjaja, *Geophys. Res. Lett.* **37**, L17306 (2010).
26. G. D. Bensen *et al.*, *Geophys. J. Int.* **169**, 1239–1260 (2007).
27. M. Barmin, M. H. Ritzwoller, A. L. Levshin, *Pure Appl. Geophys.* **158**, 1351–1375 (2001).
28. A. Mordret, M. Landès, N. M. Shapiro, S. Singh, P. Roux, *Geophys. J. Int.* **198**, 1514–1525 (2014).
29. T. M. Brocher, *Bull. Seismol. Soc. Am.* **98**, 950–968 (2008).
30. K. Wohletz, G. Heiken, *Volcanology and Geothermal Energy* (Univ. of California Press, Berkeley, CA, 1992).
31. E. Chaussard, F. Amelung, *Geophys. Res. Lett.* **39**, L21311 (2012).

ACKNOWLEDGMENTS

All of the data used in this study (doi:10.14470/2N934755) were acquired with instruments from the GFZ instrument pool (GIPP) and distributed by the GFZ-GEOFON data center. Computations in this study were performed using the High-Performance Computing infrastructure S-CAPAD at the Institute de Physique du Globe de Paris, which is supported by the Île-de-France region (via the SEASAME program), France-Grille (http://www.france-grilles.fr), and the CNRS MASTODONS program. The work of K.J., A.M., and N.M.S. was supported by the European Union through the European Research Council advanced grant project 227507 Whisper and for C.S.-S. by the Federal Ministry of Education and Research (BMBF) project MIIC (grant no. 03G0736A). I.K. was supported by the Russian Science Foundation (grant no. 14-17-00430). M.L. was supported by the French project DataScale. We acknowledge C. Jaupart (Institut de Physique du Globe de Paris) for helpful discussions.

SUPPLEMENTARY MATERIALS

www.sciencemag.org/content/346/6209/617/suppl/DC1
Materials and Methods
Figs. S1 to S10
Table S1
References (*32*–*43*)

10 July 2014; accepted 1 October 2014
10.1126/science.1258582